

Valence bands of AgCl and AgBr: uv photoemission and theory

J. Tejada, N. J. Shevchik, W. Braun, A. Goldmann,* and M. Cardona
Max-Planck-Institut für Festkörperforschung, Stuttgart, Federal Republic of Germany
 (Received 29 October 1974)

AgCl and AgBr have been investigated by photoemission for photon energies $h\nu = 16.8, 21.2, 26.9, 40.8,$ and 1486.6 eV. By exploiting the strong dependence on $h\nu$ of the photoionization cross sections for the atomic orbitals composing the valence bands, we have been able to deduce approximate partial p and d densities of valence states for these compounds. The most conspicuous feature of the photoelectron distribution curves is a sharp peak near the center of the valence band, which our partial density of states shows to be mostly d -like. The p density of states exhibits two main peaks centered at 2- and 5-eV binding energy and a gap at the energy of the sharp d peak. From the p and d densities of states we conclude that, except for the sharp d -like peak and the associated p gap, the p and d functions are nearly equally and uniformly mixed throughout the valence band. The results are compared with partial densities of states calculated with a simplified tight-binding scheme and the band structure is discussed in detail.

I. INTRODUCTION

Throughout this paper, we consider the wave functions of the valence bands of the materials under study (AgCl, AgBr) as composed of linear combinations of atomic orbitals of the constituent atoms in the spirit of the tight-binding approximation. When using photoelectron spectroscopy to study densities of valence states, that fact introduces considerable complications since for a given exciting photon energy, different atomic orbitals have, in general, different excitation cross sections.¹⁻³

The observed "density of states" are actually considerably deformed, due to variations in orbital composition across the bands. This fact can, however, be exploited by measuring the energy distribution curves of photoelectrons emitted with exciting photons of different energies, provided the energy dependence of the excitation cross sections of the atoms or ions involved is known.^{3,4} Under these circumstances, it is possible to extract from the data not only the undistorted density of states but also the partial densities of states for each atomic orbital.

Information about partial densities of states is also obtained in soft-x-ray emission spectroscopy (SXS).^{5,6} When a valence electron falls into a core hole, dipole-selection rules must be obeyed for strong-x-ray emission to result. Thus if the hole has orbital angular momentum l , only those orbital components of the valence bands with angular momentum $l \pm 1$ will be seen. The resolution of the SXS technique, however, is limited by the intrinsic width of the core levels involved, which can be as much as 5 eV (typically ~ 1 eV).

This problem does not seem to appear as serious in x-ray and in uv-photoelectron spectroscopy where the resolution limit is set by the linewidth

of the exciting source and by the electron energy analyzer. A resolution of 1.2 eV is reached with the conventional unmonochromatized Al- $K\alpha$ source. The use of an x-ray monochromator reduces the width of the source to about 0.5 eV. With a uv source, either synchrotron radiation or gas discharge lamps, the resolution is determined by the energy analyzer and can be made as small as 0.1 eV for solid-state studies.

AgCl and AgBr crystallize in the rock-salt structure and thus differ considerably from AgI and the copper halides (zinc blende). All of these materials are characterized by the presence of d orbitals ($3d$ in Cu, $4d$ in Ag) in the energy region of the valence bands. These d orbitals are intimately mixed with the p valence wave functions of the halogen.

Band calculations for these materials cannot be performed by the usual local-pseudopotential method; however, they can be incorporated with a non-local angular-momentum-dependent pseudopotential.⁷ Using a mixed basis set of linear combination of atomic orbitals (LCAO) and plane waves, Fowler⁸ calculated the band structures of AgCl and AgBr and their dependence on lattice constant. Scop⁹ calculated the band structures of these materials with the augmented-plane-wave (APW) method. Bassani *et al.*¹⁰ calculated the band structure of AgCl with the tight-binding method but argued that the valence-band width should be twice as large as the calculated one and derived a "speculative" band structure (essentially a rescaled version of their previously calculated one) which was in agreement with the experimental data available at that time. A somewhat consistent picture of these band structures has been provided by these calculations. The main difference between AgCl and AgBr and their tetrahedral counterpart (AgI) is due to the inversion symmetry of rock

salt. The valence states at Γ ($\vec{k}=0$) must have definite parity and thus are either pure p of the halogen (Γ_{15}), d of the metal ($\Gamma_{25}'; \Gamma_{12}$), or s of the halogen (Γ_1). The top valence state at $\vec{k}=0$ is actually a pure p -halogen state. Off $\vec{k}=0$, the p (halogen) and d (metal) states, which are approximately 1 eV below the p -halogen levels, begin to mix very heavily, and a strong repulsion between the upper p and d bands takes place. As a result, the highest valence-band maximum occurs off the center of the zone, and the materials have indirect absorption edges. Until recently, even though the silver halides had been extensively studied by optical absorption and reflection (see, for example, Refs. 10–13), the position and degree of banding of the Ag $4d$ levels had not been determined accurately. Bauer and Spicer¹⁴ and more recently, Williams *et al.*¹⁵ found sharp peaks in the electron-energy distribution curves (EDC's) at ~ 3 eV, which they attributed to unhybridized d levels, while other portions at higher energy were hybridized. Bauer and Spicer also found an anomalously large temperature dependence of the EDC's, which they attributed to changes in hybridization with thermal motion of the ions.¹⁵

The recent work of Mason¹⁶ with monochromatized x rays suggests that the speculative band structure of Bassani *et al.*¹⁰ is in agreement with experiments and that the temperature dependence of the EDC's is much less than that measured by Bauer and Spicer at lower photon energies.¹⁴ Because of the limitation of a single excitation energy, the partial and total densities of states were not extracted from these EDC's. In fact, for the x-ray excitation, the EDC's are primarily determined by the partial d density of valence states.³

We have measured the photoemission spectra of AgBr and AgCl with the Ne and He resonance lines ($h\nu=16.8, 21.2, 26.9, \text{ and } 40.8$ eV). By exploiting the dependence of the photoionization cross section upon photon energy, we have deduced the partial p , d , and the total densities of valence states. Unfortunately, to our knowledge, no density-of-states calculation is available for comparison with our experimental results. We have therefore calculated the band structure and partial density of states from a simplified parametrized tight-binding model which retains only nearest-neighbor interactions. In addition, we have reduced much of the secular equation by hand to obtain analytical solutions along some symmetry directions. We discuss the details of the band structure, and in particular, which features give rise to the observed peaks in the densities of valence states.

II. CALCULATIONS

In this section, we describe a tight-binding model for the valence bands of AgCl and AgBr. This

model contains a minimum number of basis functions and parameters. Our purpose is not to make a first-principles calculation, such as in the earlier work of Scop⁹ and Bassani *et al.*,¹⁰ but rather to determine an empirical band structure by fitting our model to experiment in order to see which interactions give the densities of states their particular shape. The model is general enough to describe approximately all rock-salt materials in which only the cation d and anion p orbitals are important in forming the valence band.

We list the energies of the outermost atomic orbitals of Ag, Cl, and Br as calculated by Herman and Skillman¹⁷ in Table I. The energy of the s orbital of the anion lies 15 eV below those of the p and d orbitals, and thus this s orbital should not strongly influence the upper valence bands. The Ag $5s$ orbital, which constitutes the lowest conduction band, is only about 6 eV above the p and d orbitals and should have a much stronger influence on the p - d derived valence bands than the halogen s orbitals. We therefore neglect the halogen s orbital and keep the Ag $5s$ orbital in our model. This is in contrast to the work of Bassani *et al.*,¹⁰ in which the halogen s orbital was retained and the Ag $5s$ orbital neglected. Since the spin-orbit splitting of the atomic Ag $4d$ orbital (0.65 eV) (Ref. 17) is much smaller than the observed d band width, a nonrelativistic calculation should suffice to explain the observed features in the density-of-valence states (DOVS). In order to keep the number of parameters small, we extend the matrix elements to nearest-neighbor atoms only and assume orthogonality of the orbitals. The ultimate test of this approximation will be determined by the success of the model in fitting the experimental density-of-valence states. The functional behavior of the atomic orbitals near the atomic origins is

$$s: 1, \quad p: x, y, z,$$

$$dt_{2g}: xy, xz, yz,$$

$$de_g: 3(x^2 - y^2), 2x^2 - x^2 - y^2.$$

We note that in a cubic environment, the five d

TABLE I. Binding energies of the atomic states involved in the valence bands of AgBr and AgCl according to Herman and Skillman (Ref. 17).

Orbital	Energy (eV)
Cl 3s	-28.5
Cl 3p	-12.2
Br 4s	-23.4
Br 4p	-11.2
Ag 5s	-6.4
Ag 4d	-12.7

levels split into two groups: e_g (doublet) and t_{2g} (triplet). By inspection of a suitably labeled prim-

itive cell, we obtain for the above functions the following Hamiltonian matrix:

$$\begin{array}{cccccccc|c}
 E_s & V_{spx} & V_{spy} & V_{spz} & 0 & 0 & 0 & 0 & 0 \\
 V_{spx}^* & E_p & 0 & 0 & V_{rx} & V_{rz} & 0 & V_{ox} & -\frac{1}{\sqrt{3}}V_{ox} \\
 V_{spy}^* & 0 & E_p & 0 & V_{rx} & 0 & V_{rz} & -V_{oy} & -\frac{1}{\sqrt{3}}V_{oy} \\
 V_{spz}^* & 0 & 0 & E_p & 0 & V_{rx} & V_{ry} & 0 & \frac{2}{\sqrt{3}}V_{oz} \\
 0 & V_{rx}^* & V_{rx}^* & 0 & E_d & 0 & 0 & 0 & 0 \\
 0 & V_{rz}^* & 0 & V_{rx}^* & 0 & E_d & 0 & 0 & 0 \\
 0 & 0 & V_{rz}^* & V_{ry}^* & 0 & 0 & E_d & 0 & 0 \\
 0 & V_{ox}^* & -V_{oy}^* & 0 & 0 & 0 & 0 & E_d & 0 \\
 0 & -\frac{1}{\sqrt{3}}V_{ox}^* & -\frac{1}{\sqrt{3}}V_{oy}^* & \frac{2}{\sqrt{3}}V_{oz}^* & 0 & 0 & 0 & 0 & E_d
 \end{array} ,$$

where

$$V_{spj} = 2iV_{sp} \sin \frac{1}{2}k_j ,$$

$$V_{rxj} = -2iV_{dpr} \sin \frac{1}{2}k_j ,$$

$$V_{oj} = 2iV_{dps} \sin \frac{1}{2}k_j .$$

k_j is the reduced wave vector, and j labels the coordinates x , y and z . (One could also obtain this result from the general expressions given by Slater and Koster¹⁸).

In this Hamiltonian, there are six adjustable parameters: E_s , E_p , E_d , V_{sp} , V_{dps} , V_{dpr} . Since the e_g levels have their charge density directed towards the nearest neighbors, they participate in σ -type bonding with the p levels. The t_{2g} levels, however, have a vanishing charge density in the direction of the nearest neighbors, but can participate in the weaker π -type bonding with the anion p levels. Thus we expect $|V_{dps}|$ to be greater than $|V_{dpr}|$. We further assume that the t_{2g} and e_g levels are not split by the octahedral environment. Fowler and Scop found this splitting to be no more than a few tenths of an electron volt.^{8,9}

The total and partial densities of states were computed by diagonalizing the full 9×9 matrix at 150 points in the reduced zone. A linear interpolation scheme was used to increase the effective resolution to 0.2 eV.

The analytical solutions for the energy bands along the Δ , Σ , and Λ axes are given in Table II. The Λ_3 , Σ_4 , Σ_3 , and Δ_5 bands are derived from the p and d orbitals and are symmetric about the average energy \bar{E} . The singlet bands having Λ , Σ , and Δ symmetry are derived from s , p , and d levels

and are found as solutions to the 3×3 secular equations.

III. EXPERIMENT

The uv measurements and the determinations of the binding energies of core levels were performed with a Vacuum Generator's ESCA III system,

TABLE II. Eigenvalues along the Λ , Δ , and Σ axes for the model Hamiltonian. $\Delta E = E_d - E_p$, $\bar{E} = \frac{1}{2}E_d + E_p$.

Symmetry	
Λ_3	$\bar{E} \pm \frac{1}{2}[\Delta E^2 + 4(V_{rx}^2 + 2V_{ox}^2)]^{1/2}$
Σ_3	$\bar{E} \pm \frac{1}{2}(\Delta E^2 + 8V_{rx}^2)^{1/2}$
Σ_4	$\bar{E} \pm \frac{1}{2}(\Delta E^2 + 8V_{ox}^2)^{1/2}$
Δ_5	$\bar{E} \pm \frac{1}{2}(\Delta E^2 + 4V_{rx}^2)^{1/2}$

s , p , d singlet band matrices along the Λ , Σ , and Δ axes

$$\begin{array}{l}
 \Lambda_1: \begin{pmatrix} E_s & \sqrt{3}V_{spx} & 0 \\ \sqrt{3}V_{spx}^* & E_p & 2V_{rx} \\ 0 & 2V_{rx}^* & E_d \end{pmatrix} \\
 \Sigma_1: \begin{pmatrix} E_s & \sqrt{2}V_{spx} & 0 \\ \sqrt{2}V_{spx}^* & E_p & \sqrt{2}(V_{rx} + \frac{i}{\sqrt{3}}V_{ox}) \\ 0 & \sqrt{2}(V_{rx}^* - \frac{i}{\sqrt{3}}V_{ox}) & E_d \end{pmatrix} \\
 \Delta_1: \begin{pmatrix} E_s & V_{spx} & 0 \\ V_{spx}^* & E_p & \frac{\sqrt{4}}{3}V_{ox} \\ 0 & \frac{\sqrt{4}}{3}V_{ox}^* & E_d \end{pmatrix}
 \end{array}$$

equipped with both a differentially pumped capillary cold cathode gas discharge lamp and an unmonochromatized Al- $K\alpha$ x-ray source. The monochromatized x-ray study of the valence band was done with a Hewlett Packard 5950 ESCA Spectrometer. In all cases, the samples were evaporated from single crystals in the preparation chamber. The base pressure during evaporation was better than 10^{-7} Torr. It was found, particularly for AgBr, that a long evaporation (100 sec) at a temperature close to the melting point caused the preferential evaporation of the halide leading to a silver-rich residue on the boat, as determined by its metallic shine. In this case, x-ray core level spectra showed that the deposited sample was also silver rich. A plausible explanation of this effect is that heating causes decomposition of the source material and that the halogen has a lower sticking probability than the silver. After the source has lost sufficient halogen, the deposit becomes silver rich. This problem was eliminated by evaporating for a short time (20 sec) at a higher temperature. The film thickness was estimated to be ~ 10000 Å. The measurements were made at room temperature at a pressure better than 10^{-4} Torr. The cleanliness of the samples was checked by measuring the x-ray spectrum at the beginning and at the end of each run. No trace of either carbon or oxygen could be detected, a fact which indicates a contamination of less than 0.1 of a monolayer (or less than 2% of the sampled volume).

The resolution of the measurements with monochromatized x-rays reported here is better than 0.8 eV. For the He I and Ne I spectra, the instrumental resolution is 0.1 eV, while for He II and Ne II it is 0.3 eV.

IV. RESULTS

A. Experiment

The EDC's of AgCl obtained with Ne I (16.8 eV), He I (21.1 eV), Ne II (26.9 eV), He II (40.8 eV), and monochromatized Al $K\alpha$ (1486.6 eV) are presented in Fig. 1. The estimated contribution of secondary electrons is indicated by the dashed line. The Ne II spectrum, corrected for the contribution due to a satellite line at 27.8 eV that has 20% the intensity of the main line, is also plotted (dashed line). The main features are observable in all the spectra. The Ne I curve may show some final density of states and/or direct-transition effects, due to the rather small exciting energy. The data obtained with Ne II are not as reliable as the others, due to the satellite correction; nevertheless, it clearly shows an intermediate step in the dependence of the cross section on photon energy between He I and He II. The corresponding results for AgBr obtained with He I, He II, and mono-

chromatized Al- $K\alpha$ x-rays are shown in Fig. 2. The He II spectra of both compounds closely resemble the results of Williams *et al.*¹⁵ The XPS data are similar to those of Mason.¹⁶ As discussed in V in more detail, the valence bands of AgCl and AgBr are composed of the halogen p and s states and the Ag $5s$ and $4d$ states. From x-ray photoelectron spectra (not shown in Figs. 1 and 2), the (halogen) s bands are found to be situated at binding energies (referred to top of valence band) of 14.3 ± 0.6 eV in AgCl and 14.8 ± 0.6 eV in AgBr. Since they are well separated from the upper valence band, which ends at about 6 eV binding energy, the halogen s levels are not expected to mix strongly with them. Furthermore, the excitation cross sections for s -like states of Cl^- and Br^- are negligible^{19,20} compared to p - and d -like contributions in our uv photon-energy range.^{20,21}

As discussed at length elsewhere,³ the EDC's corrected for inelastic electrons, escape depth, and analyser transmission can be expressed as

$$N(E, h\nu) = \rho_p(E)\sigma_p(h\nu) + \rho_d(E)\sigma_d(h\nu), \quad (1)$$

where $\rho_{p,d}(E)$ are partial p and d densities of

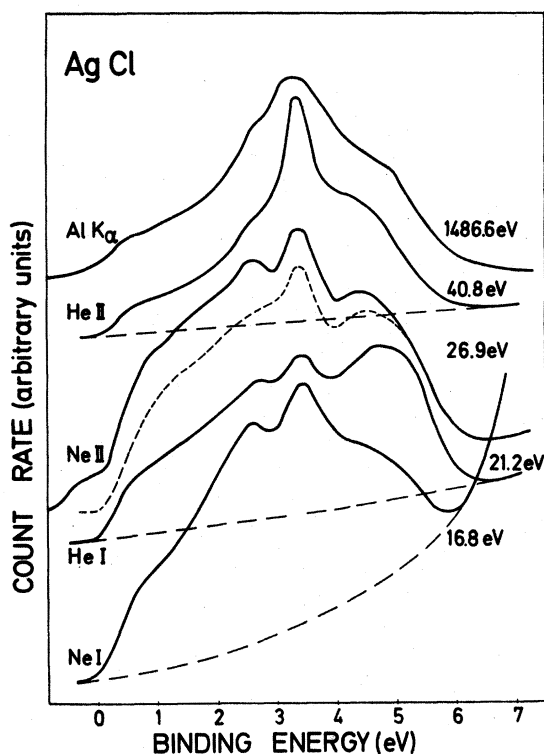


FIG. 1. Energy distribution curves (EDC's) for AgCl obtained with 16.9, 21.2, 26.9, 40.8, and 1486.6 eV radiation. The estimated contribution from secondary electrons is shown with a long-dashed line. Also shown with a short-dashed line is the Ne II EDC with the contribution from a satellite line at 27.8 eV subtracted.

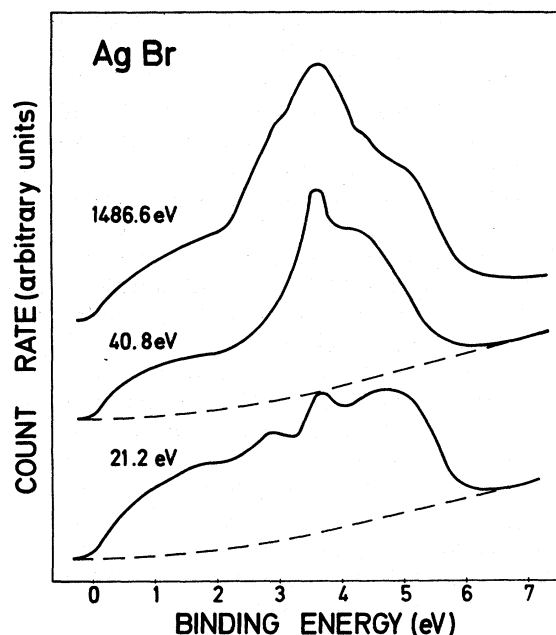


FIG. 2. EDC's for AgBr obtained with 21.2, 40.8, and 1486.6 eV radiation. The estimated contribution from secondary electrons is shown with a dashed line.

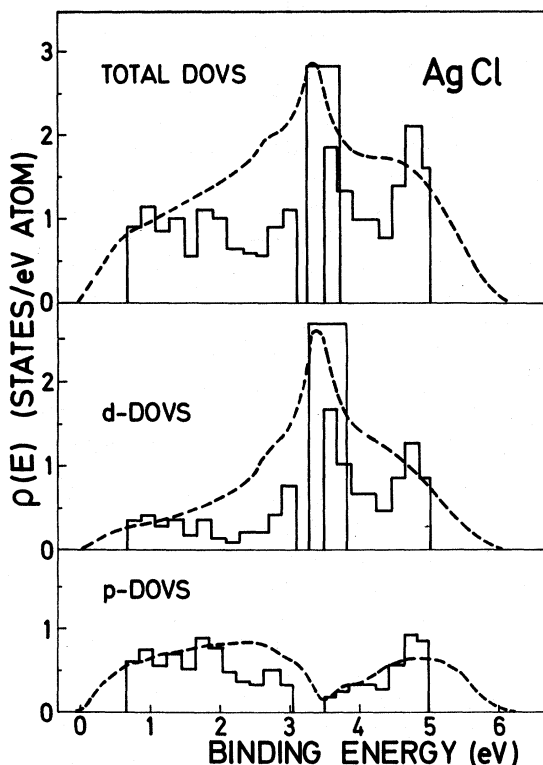


FIG. 3. Comparison of theoretical and experimental density of valence states for AgCl. The total and partial p and d DOVS were obtained from the He I and He II EDC's of Fig. 1 (see text).

states, and $\sigma_p(h\nu)$ and $\sigma_d(h\nu)$ are the corresponding photoionization cross sections per electron at the photon energy $h\nu$. It can be shown⁴ that the contribution to the total cross section, due to interference between the hybridized wave functions on neighboring atoms, neglected in Eq. (1), is negligible in the considered kinetic-energy range of the photoemitted electrons.

We have also assumed that the cross section does not depend upon the energy of the critical state (see below). The total photoionization cross section for Ag metal,²¹ which represents to a very good approximation the Ag $4d$ contribution, and the experimental $3p$ and $4p$ subshell cross sections of Cl^- and Br^- (Ref. 20) have been determined experimentally as a function of wavelength. We can therefore treat two EDC's taken at different exciting energies as two linearly independent equations for the p and d partial DOVS [see Eq. (1)]. By assuming that there are a total of 10 d and 6 p electrons in the valence band, we can obtain the properly normalized $\rho_d(E)$ and $\rho_p(E)$ and thus the total DOVS. Using the EDC's obtained with 21.2 and 40.8 eV, and taking the values of the cross sections $\sigma_p(3p, 4p)$ and $\sigma_d(4d)$ at the same photon energies from Refs. 20 and 21, respectively, we can separate the contributions of $\rho_p(E)$ and $\rho_d(E)$ to the EDC's and thus finally obtain the partial p and d and the total DOVS's shown in Figs. 3 (dashed line) and 4. We also compare in Fig. 3

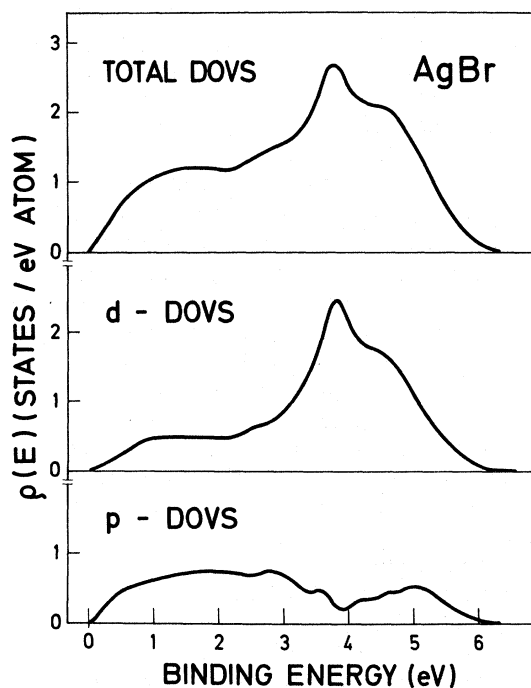


FIG. 4. Total and partial p and d DOVS for AgBr obtained from Fig. 2 (see text).

these densities of states with those calculated from our band model for AgCl (see discussion).

Before comparing our experimental DOVS's with theory, it is appropriate to discuss their accuracy. The most serious approximation made in extracting the DOVS's from the photoemission data is the assumed independence of the cross sections on the initial state energy. For the He II spectrum, the p and d cross sections vary little over the band widths, and they should be accurately described by the Eq. (1). Since the d cross section is an order of magnitude greater than the p cross section at this energy, the He II spectrum already yields a d DOVS to at least 10% accuracy. The correction made due to the small p -like contribution should improve the accuracy of the d DOVS to better than 5% at every point. For the He I spectrum, the d cross section varies little over the band width, but the p cross section, as suggested by the calculations of Kennedy and Manson²² and Fano and Cooper,²³ might vary as much as $\pm 20\%$ at the end points. This variation would tend to distort the p -like DOVS by exaggerating the structure at the bottom of the band. One possible way to estimate this error would be to do this analysis using EDC's excited with different energies; however, the only experimental cross sections available are those at 21.1 and 40.8 eV. Trying different combinations of the 26.9- and the 40.8-eV EDC's, a partial p DOVS was obtained in good agreement with the one shown in Fig. 3, suggesting that the variation of the cross section over the band is not distorting the spectra significantly. The p DOVS is probably determined to an accuracy of about 10% at the average point, depending upon the accuracy of the cross sections used.

The agreement of the EDC's taken with He II and Al $K\alpha$ demonstrates that the EDC's are not dependent on escape depths, and therefore the contribution of any surface states are unimportant. The partial d DOVS's clearly show peaks positioned with respect to the top of the valence band at 3.4 ± 0.1 and 3.8 ± 0.1 eV for AgCl and AgBr, respectively, in agreement with Bauer and Spicer's values of 3.3 and 3.7 eV and Williams' *et al.* data of 3.5 and 3.8 eV.^{14,15} Since the p DOVS's have minima at these energies, these peaks are primarily d -like. A determination of the number of electrons associated with these peaks is somewhat arbitrary since their base is broad and overlaps with the portions that are involved in hybridization. Our theoretical curves give two electrons per molecule under this peak. Bassani *et al.*¹⁰ as well as Scop⁹ predict a flat d -like band at approximately the same energies in their calculations. They differ in their assignments of the symmetry for these states: Bassani *et al.*¹⁰ attribute $\Gamma_{25'}$ symmetry to them, whereas Scop⁹ assigns them Γ_{12} sym-

metry. In Subsec. B, we shall show that this peak is a mixture of both types of d states because the band repulsion between the p and d states is much larger than the $\Gamma_{25'} - \Gamma_{12}$ crystal-field splitting. It corresponds to a flat band arising from the fact that the 3 p function can repel only 3 of the 5 d functions. The strong p - d repulsion causes a gap in the p DOVS. The p DOVS of Figs. 3 and 4 indicate that the p levels mix with nearly equal strengths on both sides of the p gap (d peak). Aside from the sharp d -like peak, the remaining d states appear to be well mixed with the anion p levels.

The observed density of states is somewhat wider than calculated, probably due to intrinsic lifetime broadening rather than instrumental resolution. The most glaring discrepancy between theory and experiment is in the sharpness of the leading edge of the EDC's; theory predicts a sharp edge, but experimentally, it is observed to be much more rounded than can be attributed to instrumental resolution. An abrupt edge is expected since the top of the valence band occurs at a multiple point of high density of states at the edge of the zone. This is in contrast to zinc-blende materials where the top of the valence band occurs at Γ_{15} , a point of small density of states. The round edge might be related to the large thermal broadening observed by Bauer and Spicer¹⁴; it could also be due to final-state effects, in which the solid responds to the presence of the hole potential created by the emitted electron. Citrin *et al.*²⁴ have suggested that phonon cascades created in response to the hole potential lead to a broadening of core levels by as much as 1 eV. Similar effects might be produced by valence band holes. Additional broadening might occur because of the variation in the Madelung energy at the surface. Such a variation would have a strong influence on the EDC's when the electron escape depth is only a few atomic layers, as it is in uv photoemission.

Core level energies determined for some Ag levels in AgCl, AgBr, and Ag metal are given in Table III. These binding energies are referred to the top of the valence band for the compounds and to the Fermi level for the metal. For the purpose of comparison, all binding energies should be referred to the vacuum level. This requires a knowledge of the photoelectric threshold Φ . (The photoelectric threshold was determined from the position of the low-energy cutoff of the EDC's. The threshold energy is $h\nu - W$, where W is the separation between the cutoff and the top of the valence band.) From our uv measurements, we find $\Phi = 6.3 \pm 0.3$ for AgCl and AgBr and 4.4 ± 0.3 for Ag metal, in agreement with the values $\Phi = 6, 6,$ and 4.3 eV given for the same quantities in Ref. 25. The energy difference between the Fermi level (ob-

TABLE III. Binding energies of Ag core electrons. All errors are ± 0.1 eV unless otherwise stated. The energies are referred to the top of the valence band for the compounds and to the Fermi level for the metal. The bottom row of the Table give the photoelectric threshold Φ with respect to the top of the valence band, as determined in this work.

Ag level	AgCl	AgBr	Ag metal
$3p_{1/2}$	601.9	602.0	604.0
$3p_{3/2}$	571.0	571.3	573.2
$3d_{3/2}$	372.3	372.4	374.3
$3d_{5/2}$	366.1	366.4	368.3
$4s_{1/2}$	94.9(3)	94.9(3)	96.8
Φ (eV)	6.3(3)	6.3(3)	4.4(2)

tained by calibration with the evaporated Ag sample) and the top of the valence bands δE has been measured to be $\delta E = 1.3(2)$ eV for AgCl and $1.3(2)$ eV for AgBr. Within the given errors, these numbers are the same for ultraviolet measurements (21.2 eV) and x-ray (1486.6 eV) measurements at different intensities. Williams *et al.*¹⁵ determined the position of the Fermi level above the top of the valence band to be 1.7 eV for AgCl and 1.1 eV for AgBr. The differences with our values might be due to charging effects or different doping or nonstoichiometry of the samples. According to Ref. 25, the energy gap is 3 eV for AgCl and 2.5 eV for AgBr; hence, the Fermi level is situated approximately in the middle of the gap, as expected for intrinsic samples without surface states. From the data given above, we conclude that for the evaporated samples used in our experiments, charging effects are very small (< 0.2 eV). Using our values (see Table III), we find that with respect to the vacuum level all Ag levels have the same binding energy (within ± 0.3 eV) in both the halides and the metal. This is a surprising result considering the high-ionic character of the bond [Phillips' ionicity is 0.850 for AgBr and 0.856 for AgCl Ref. 26]. We discuss these chemical shifts in terms of a simplified charge-transfer model in Sec. VII.

B. Band structures

In the first band structure attempted, the energies of the atomic orbitals as given by Herman and Skillman¹⁷ were used. (We do not expect the atomic-energy values as calculated by Herman and Skillman¹⁷ to be exactly correct for the solid, where Madelung terms can shift them.) The strength of the π bonding was at first taken to be $\frac{1}{2}$ of that of the σ bonding, and the parameters were fit to match the 3.2 eV indirect gap between L_3 and Γ . The s - p interaction was chosen to fit the

TABLE IV. Comparison of the interaction parameters used here with those of Bassani *et al.* (Ref. 10). The zero-energy point has been chosen to correspond to the Cl $3p$ level in both cases.

Parameter	This work	Bassani <i>et al.</i>
$E_{Ag s}$	+4.8	...
$E_{Cl p}$	0.0	0.0
$E_{Ag d}$	-1.2	-1.3
V_{sp}	-1.2	...
$V_{dp\sigma}$	-0.7	-1.24
$V_{dp\pi}$	+0.2	0.38

6-eV L_3 - L_2 splitting observed in the optical data.¹³ The shape of the resulting band structure was in fair agreement with those of Bassani *et al.*¹⁰ and Scop,⁹ and the total bandwidth is in good agreement with the photoemission experiments reported here. However, this band structure gave a density of states in which the lower d valence bands were too wide. To remedy this situation, we increased the energy of the p level by 1 eV to account for Madelung corrections and decreased the bonding parameters to keep the band gap correct. We also found that using $V_{pd\pi} = -0.3 V_{pd\sigma}$, a value similar to that found by Bassani *et al.*,¹⁰ gave better agreement with experiment. The adjusted band structure is shown in Fig. 5, and the corresponding DOVS has already been compared with experiment in Fig. 3. A comparison of the parameters used here to those of Bassani *et al.*¹⁰ is shown in Table IV. The primary change in the band structure with this adjustment is the desired narrowing of the lower portions of the DOVS, while the upper portions retain their previous width. The p - d interaction parameters used here are about half of those used by Bassani *et al.*,¹⁰ but our bandwidth (4.3 eV) is greater than theirs (3.2 eV). The agreement with the band structure of Bassani *et*

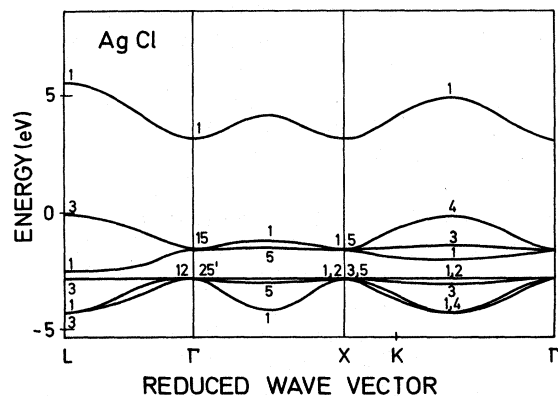


FIG. 5. Empirical tight-binding band structure for AgCl. The zero energy has been shifted to correspond to the top of the valence band.

*al.*¹⁰ as interpreted by Mason¹⁶ is very good, especially with regard to the features along the Δ axis. (Inclusion of charge-density overlap would also tend to narrow the lower bands relative to the upper bands.)²⁷

V. DISCUSSION

As seen in the band-structure calculations, the origin of the sharp d -like peak in the experimental and theoretical DOVS is due to two flat d bands that occur at the energy of the atomic d level. In our model Hamiltonian, the five degenerate d levels couple to only the three degenerate anion p levels. We are, of course, free to take any linear combination of the $5d$ levels to achieve a

state of vanishing interaction with all of the p levels. Since five coefficients are needed to define a d state and there are only three constraints to satisfy (i. e., $\langle d|H|p\rangle=0$), two such pure d states can always be constructed. This result is independent of the actual values of the matrix elements and thus hold for an arbitrary point in k space. These two d levels produce flat bands and thus δ functions in the DOVS. As long as every Ag atom is surrounded by Cl atoms, so that there are no d - d interactions, this peak should be insensitive to structure (applies to tetrahedral structures, too) or to phonon broadening.

From the secular equation, we find that one of the unhybridized d states for a general point in k space is given by

$$\psi = V_{dp\sigma}[(\sin^2 k_x + \sin^2 k_y)(\sin k_x d_{xy} + \sin k_y d_{xz}) + (\sin^2 k_x - \sin^2 k_y) \sin k_z d_{xy}] + V_{dp\pi}(\sin k_x \sin k_y \sin k_z) d_{x^2-y^2}.$$

As can be seen from the above expression, this state is a mixture of the t_{2g} and e_g orbitals. Without doing a full k -space integration, we estimate the fraction of the e_g to t_{2g} contribution to be given approximately by the ratio of the average of the square of their weighting coefficients or

$$f_{eg}/f_{t_{2g}} \cong \frac{1}{3}(V_{dp\pi}/V_{dp\sigma})^2. \quad (2)$$

Since

$$|V_{dp\pi}| \leq \frac{1}{2} |V_{dp\sigma}|,$$

the contribution from the e_g level is at most 10%. In the limit where the π bonding vanishes, the three t_{2g} levels produce flat bands and the δ function in the density of states contains 3 electrons.

We wish to stress that this peak does not arise because the d states are corelike in the sense that they are so localized about the nucleus that their overlap with the p levels vanishes; the interaction is zero because a phase cancellation of the matrix elements can always be achieved, since there are more d orbitals than p orbitals.

The above argument holds rigorously only with the assumptions built into our Hamiltonian. Bassani *et al.*¹⁰ have estimated that the second-neighbor d - d interactions are only 0.01 eV, and thus we do not expect them to influence the width of the unhybridized d bands. Spin-orbit and crystal-field interactions, which remove the $t_{2g} - e_g$ degeneracies, would broaden this peak. Inclusion of the anion s level would provide another constraint (in addition to the three provided by the anion p levels), so that only one flat band can be constructed. Even in the presence of the anion s level, it can be shown that the t_{2g} orbitals produce a flat band over the $k_z=0$ and $k_x=\pi$ planes in the reduced zone, an

area sufficiently large to produce a peak in the DOVS.

To discuss the other features of the DOVS, it is necessary to inspect the band structure and the matrix in more detail.

Along Λ , the repulsion between the p - and d -derived Λ_3 bands of Table II is large, because the π and σ bonding are used to the maximum possible. There is also a flat set of Λ_3 bands which corresponds to the unmixed d levels discussed earlier (see Fig. 5). The upper and lower singlet bands result from a strong s - p interaction, which is also a maximum along this direction. The s - p repulsion in this direction is primarily responsible for the filling in of the gap between the p and d density of states by the middle singlet band.

Along Δ , the repulsion between the Δ_5 bands is weak, since only π -type interaction between the p and d levels is involved. The lower two singlet bands repel one another more strongly since σ bonding is involved and is the greatest along this axis. Thus, in general, we might expect the Δ_1 band to lie higher than the Δ_5 band, in agreement with the band structures of Bassani *et al.*,¹⁰ and Scop.⁹ However, the middle X band does not arise nearly as high in energy as in the calculation of Bassani *et al.*, due to the downward repulsion from the upper Ag s -like band. At the X point, all levels return to their atomic values, because in this model all interactions vanish. Inclusion of more basis functions and interactions with more distant neighbors would alter the situation. Because of the strong bonding, the p - d bands repel one another along Σ almost as strongly as in the Λ direction. The Σ_3 bands repel each other less since only π -type interaction is involved. For the singlet bands, the s - p interactions are somewhat

weaker than for the Λ direction, and the corresponding p - d interaction is due to the weaker π interaction. In contrast to the work of Bassani *et al.*,¹⁰ the middle Σ_1 band falls below the upper Σ_3 band as a consequence of the repulsion from the upper Ag s -like band. Because the energy bands depend strongly on the direction of the k vector, no pronounced features occur in the density of states other than from the flat d bands. This is in contrast to the zinc-blende materials where the spherically isotropic bands produced pronounced peaks in the DOVS.

It is of interest to determine which point in the valence bands lies the highest. As seen from Table II, among the pure p - d bands, the L_3 point lies the highest, the point midway along the Σ_4 band lies the next highest, and Δ_5 band lies the lowest. The reason for this is that for the sequence L_3 , Σ_4 , Δ_5 , the stronger σ bonding gives way to the weaker π bonding. When the repulsion from the upper Ag $5s$ level is weak, it is easily seen that the Δ_1 band can lie higher than the Δ_5 but never higher than the L_3 and Σ_4 band maxima. Using the expressions in Table II, we find that the separation between the maxima in the L_3 and Σ_4 bands is given by

$$E_{L_3} - E_{\Sigma_4} \cong (V_{dp\sigma})^2 / 2^{1/2} |V_{dp\sigma}|. \quad (3)$$

For the parameters used in this calculation, we find that this difference is less than 0.1 eV. Scop⁹ finds that for AgCl, the L_3 maximum lies above the Σ_4 maximum, but that this ordering is reversed in AgBr; in both cases the maxima lie within 0.2 eV of one another. Since Scop⁹ has included more basis functions and interactions than we have, the reversal of the level ordering can be explained. Bassani *et al.*,¹⁰ however, find that the Δ_1 band maximum lies the highest. We believe that in their calculation, this arises from a repulsion by the lowest anion s level included in their model. If they were to include the Ag $5s$ level, such as we have, this Δ_1 band would retreat to lower energy, while the Δ_3 and Σ_4 bands would remain unmoved. Within the framework of our model, the Δ_1 band can never lie higher than the Δ_3 or Σ_4 bands.

VI. ON THE "GIANT-TEMPERATURE" DEPENDENCE OF THE EDC'S

Bauer and Spicer¹⁴ explained the large-temperature dependence of the EDC's by a change in the p - d hybridization with temperature that correspondingly modulated the band-structure density of states. Fowler,⁸ after calculating the band structure as a function of lattice constant, expressed reservations concerning this interpretation. The temperature dependence observed by Mason¹⁶ with x-ray excitation was substantially smaller than that observed by Bauer and Spicer.¹⁴

We suggest that the temperature dependence of the photoionization matrix elements can explain both the observations of Bauer and Spicer and of Mason. If we think of the conduction-band state as a plane wave, the photoionization matrix element of the solid is expressible as a Fourier transform of the hybridized p - d wave function. It can be shown⁴ that the interference term occurring in the square modulus of the transition matrix element taken between the initial state (the p - d hybrid wave function) and the final state (the plane wave) is decreasing rapidly with increasing photoelectron energy. Since this term depends upon the relative spacing of the two atoms in the unit cell, it is sensitive to thermal vibrations via a Debye-Waller factor. At low-photoelectron energies (≤ 20 eV), the transition matrix element is more sensitive to thermal motion than at high-photoelectron energies, because of the large contribution from the interference term. In the limit of high-photoelectron energies, the interference terms are unimportant and changes in the EDC's are therefore primarily due to changes in the DOVS. Thus in the low final-electron-energy range, temperature dependence of the EDC's is attributable to both density of states and matrix elements, and therefore the thermal fluctuations might be larger than we would normally expect.

VII. CORE SHIFTS

We found that upon forming the compounds under consideration the core levels of the Ag atom shift by no more than 0.3 eV with respect to the vacuum level. Previously, we attempted to relate²⁸ the chemical shifts of compounds to a charge model in which

$$\Delta E_c = \{ [3A(\Gamma)/r] - \alpha/R \} \Delta q e, \quad (4)$$

where

$$A = (1 - \Gamma^2)/(1 - \Gamma^3), \quad \Delta q = (Z - 4(1 - f_i))e,$$

r and R are the interatomic spacing in the metal and compound, respectively, Z is the valence of the cation, f_i is the Phillips' ionicity,²⁶ and α is the Madelung constant, 1.74; Γ determines the thickness of an effective shell in which the valence charge and the cation are distributed. This shell has inner and outer radii Γr and r , respectively.

TABLE V. Interatomic spacing R , Phillips ionicity f_i , charge transfer Δq , and calculated core shift ΔE_c , compared to experimental core shift.

	R (Å)	f_i	Δq	ΔE_c (eV) $\Gamma = 0.5$	ΔE_c (eV) $\Gamma = 1$	ΔE_{expt}
AgCl	2.77	0.865	0.43	-1.7	≈ 0.1	+0.2
AgBr	2.89	0.850	0.40	-1.6	≈ 0.1	0.0

The chemical shifts of most semiconductors can be represented by Eq. (4) with $\Gamma = 0.5$.²⁸ This ansatz gives for AgCl and AgBr $\Delta E_c \cong -1.6$ eV (see Table V). If one assumes $\Gamma \approx 1$, i. e., an infinitesimally thin shell, shifts of the order of 0.1 eV reasonably close to the observed absence of chemical shift are then obtained. However, it

is difficult to justify the infinitesimally thin shell for Ag in which the electron transferred has s character and for which a value of $\Gamma = 0.5$ is more appropriate. Other effects neglected by this model, especially electron and lattice polarization of the hole in the final state, are probably making important contributions to the observed core-level positions.

*On leave from Fachbereich Physik, Freie Universität, Berlin, Germany.

¹K. Siegbahn, C. Nordling, G. Johansson, J. Hedman, P. F. Heden, K. Hamrin, U. Gelius, T. Bergmark, L. O. Werme, R. Manne, and Y. Baer, *ESCA Applied to Free Molecules*, 1st Ed., (Elsevier, New York, 1971).

²R. G. Cavell, S. P. Kowlaczyk, L. Ley, R. A. Pollack, B. Mills, D. A. Shirley, and W. Perry, *Phys. Rev. B* **7**, 1513 (1973).

³A. Goldmann, J. Tejeda, N. J. Shevchik, and M. Cardona, *Phys. Rev. B* **10**, 4388 (1974).

⁴W. Braun, A. Goldmann, and M. Cardona, *Phys. Rev. B* **10**, 5069 (1974).

⁵L. G. Parratt, *Rev. Mod. Phys.* **31**, 616 (1959).

⁶G. A. Nooke, *Natl. Bur. Stds. J. Res. A* **74**, 273 (1970).

⁷C. Y. Fong and M. L. Cohen, *Phys. Rev. Lett.* **24**, 306 (1970).

⁸W. B. Fowler, *Phys. Status Solidi B* **52**, 591 (1972).

⁹P. M. Scop, *Phys. Rev. A* **139**, 934 (1965).

¹⁰F. Bassani, R. S. Knox, and W. B. Fowler, *Phys. Rev.* **137**, 1217 (1965).

¹¹S. Sato, M. Watanabe, Y. Iguchi, S. Nakai, Y. Nakamura, and T. Sagawa, *J. Phys. Soc. Jpn.* **30**, 1638 (1972).

¹²N. J. Carrera and F. C. Brown, *Phys. Rev. B* **4**, 3651 (1971).

¹³J. J. White III and J. W. Straley, *J. Opt. Soc. Am.* **58**, 759 (1968); J. J. White III, *J. Opt. Soc. Am.* **62**, 212 (1972).

¹⁴R. S. Bauer and W. E. Spicer, *Bull. Am. Phys. Soc.* **14**, 1166 (1969); *Phys. Rev. Lett.* **25**, 1283 (1970); and in *Electron Spectroscopy*, edited by D. A. Shirley (North-Holland, Amsterdam, 1972), p. 569.

¹⁵D. R. Williams, J. G. Jenkin, R. C. G. Leckey, and J. Liesegang, *Phys. Lett. A* **49**, 141 (1974).

¹⁶M. G. Mason, *J. Electron. Spectrosc.* **5**, 573 (1974); and *Phys. Rev. B* **11**, 5094 (1975).

¹⁷F. Herman and S. Skillman, *Atomic Structure Calculations* (Prentice-Hall, Englewood Cliffs, N. J., 1963).

¹⁸J. C. Slater and G. F. Koster, *Phys. Rev.* **94**, 1498 (1954).

¹⁹J. W. Cooper, *Phys. Rev.* **128**, 681 (1962).

²⁰P. C. Kemeny, R. T. Poole, J. G. Jenkin, J. Liesegang, and R. C. G. Leckey, *Phys. Rev. A* **10**, 190 (1974).

²¹H. J. Hagemann, W. Gudat, and C. Kunz (unpublished).

²²D. J. Kennedy and S. T. Manson, *Phys. Rev. A* **5**, 227 (1972).

²³U. Fano and J. W. Cooper, *Rev. Mod. Phys.* **40**, 441 (1968).

²⁴P. H. Citrin, P. Eisenberger, and D. R. Hamann, *Phys. Rev. Lett.* **33**, 965 (1974).

²⁵A. H. Sommer, *Photoemissive Materials*, 1st Ed. (Wiley, New York, 1968), Chap. 3, p. 21.

²⁶J. C. Phillips, *Rev. Mod. Phys.* **42**, 317 (1970).

²⁷J. Tejeda and N. J. Shevchik (unpublished).

²⁸N. J. Shevchik, J. Tejeda, and M. Cardona, *Phys. Rev. B* **9**, 2627 (1974).